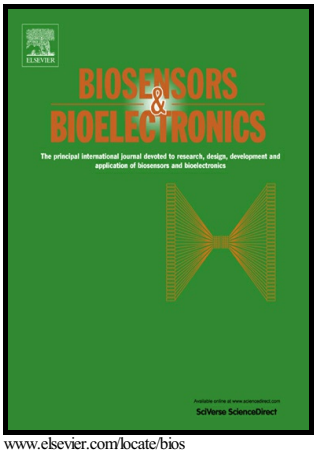

www.elsevier.com/locate/bios

Electrografting of thionine diazonium cation onto the graphene Edges and Decorating with Au Nano-Dendrites or glucose oxidase: Characterization and electrocatalytic Applications

Reza Karimi Shervedani, Akbar Amini, Nima Sadeghi

PII: S0956-5663(15)30458-9
DOI: http://dx.doi.org/10.1016/j.bios.2015.09.062
Reference: BIOS8029

To appear in: *Biosensors and Bioelectronic*

Received date: 19 July 2015
Revised date: 22 September 2015
Accepted date: 27 September 2015

Cite this article as: Reza Karimi Shervedani, Akbar Amini and Nima Sadeghi Electrografting of thionine diazonium cation onto the graphene Edges an Decorating with Au Nano-Dendrites or glucose oxidase: Characterization an electrocatalytic Applications, *Biosensors and Bioelectronic* http://dx.doi.org/10.1016/j.bios.2015.09.062

Electrografting of Thionine Diazonium Cation onto the Graphene Edges and Decorating with Au Nano-Dendrites or Glucose Oxidase: Characterization and Electrocatalytic Applications

Reza Karimi Shervedani,* Akbar Amini, Nima Sadeghi

Department of Chemistry, University of Isfahan, Isfahan 81746-73441, I. R. Iran, Corresponding author. Tel.: +98-313-7932715. Fax: +98-313-6689732. E-mail address: rkarimi@sci.ui.ac.ir (R. Karimi Shervedani).

Abstract

Thionine (Th) diazonium cation is covalently attached onto the glassy carbon (GC) electrode via graphene nanosheets (GNs) (GC-GNs-Th). The GC-GNs-Th electrode is subjected to further modifications to fabricate (i) glucose and (ii) nitrite sensors. Further modifications include: (i) direct immobilization of glucose oxidase (GOx) and (ii) electrodeposition of gold dendrite-like nanostructures (DGNs) on the GC-GNs-Th surface, constructing GC-GNs-Th-GOx and GC-GNs-Th-DGNs modified electrodes, respectively. The GC-GNs-Th-GOx biosensor exhibited a linear response range to glucose, from 0.5 to 6.0 mM, with a limit of detection (LOD) of 9.6 μM and high sensitivity of 43.2 μA cm^{-2} mM^{-1}. Also, the GC-GNs-Th-DGNs sensor showed a wide dynamic response range for NO_2^- ion with two linear parts, from 0.05 μM to 1.0 μM and 30.0 μM to 1.0 mM, a sensitivity of 263.2 μA mM^{-1} and a LOD of 0.01 μM. Applicability of the modified electrodes was successfully tested by determination of glucose in human blood serum and nitrite in water based on addition/recovery tests.

*To whom correspondence should be addressed. Tel.: +98-313-7932715. Fax: +98-313-6689732.
E-mail address: rkarimi@sci.ui.ac.ir

Keywords: Thionine; Diazonium cation; Graphene; Glucose oxidase; Gold-dendrite-like nanoparticles.

1. Introduction

Graphene nanosheets (GNs), the rapidly rising stars of carbon nanomaterials with a sp^2 hybrid carbon network, have much theoretical and experimental applications, compared to other carbon materials due to their exceptional electronic, optical, high charge mobility and large surface area properties (Geim, 2009; Li et al., 2008; Li et al., 2009; Ling et al., 2010; Novoselov et al., 2004). Functionalization, dispersion and decoration of graphene nanosheets are of crucial importance for their applications (Georgakilas et al., 2012; Kuila et al., 2012; Yin et al, 2015). To explore potential applications of graphene, several versatile methods have been established for functionalization of graphene based on reduction of diazonium salts through chemical or electrochemical grafting processes (Belanger et al., 2011; Hetemi et al., 2014; Lange et al., 2011; Wang et al., 2009).

Electrochemical grafting of organic molecules can be carried out by using various precursors such as amines, carboxylates, alcohols and diazonium salts (Belanger et al., 2011). In effect, electrografting strategies based on diazonium salts are irreversible and strong (Belanger et al., 2011; Hetemi et al., 2014). The most relevant example is direct grafting of aryl diazoniums (ArN^{2+}) to the surface. This modification procedure leads to formation of strong C–C bonds between thin films and substrates, which benefit of several advantages as thermal stability, electrochemical stability over a wide range of potentials, and possibility to introduce different functional groups at the thin films on the surface (Brooksby et al., 2005; D'Amours and Belanger, 2003; Georgakilas et al., 2012).

Thionine (Th), an artificial organic dye derivative of phenothiazine, has been widely used in photogalvanic cells and electrochemical sensors and biosensors (Deng et al. 2012; Gao et al. 2003; Ghica et al., 2015; Portaccioa et al., 2013). Usually, the Th supported onto the GNs or electropolymerized on the electrode surface (Guo et al., 2013; Zhu et al., 2012) based on non-covalent bonds, suffers from low stability and leaking from electrode surface to the bulk solution. Thus, a novel functional Th-nanomaterial should be designed to prevent effectively the leakage of the mediator and improve the stability of the biosensor.

Recently, the electrochemical reductive adsorption of aryl diazonium salts has received increasing attention (Gooding and Ciampi, 2011). Despite the advantages of this method, to the best of our knowledge, there is no report on the use of direct introduction of aryl diazonium salts onto the GNs for preparation of highly active catalysts for sensing and biosensing applications. In addition, the fabrication of gold dendrite-like nanostructures (DGNs) has been an active research area because of its morphology-dependent optical, electronic, and catalytic properties and their promising applications in sensing and biosensing (Gautham et al., 2010; Liu et al., 2013; Yin et al, 2015).

Regarding the advanced features of the GNs, Th and DGNs, herein we have developed for the first time, a new two-step electrochemical approach to synthesize a new electrocatalyst on the glassy carbon (GC) electrode. The modification is based on GNs formed by electrochemical reduction of graphene oxide (GO), and the thionine electrochemically grafted via its diazonium form onto the GC-GNs surface via GNs-Th covalent bond. Thus, GC-GNs-Th is further decorated with (i) glucose oxidase (GOx) and (ii) DGNs through electrostatic attraction and covalent interaction to construct GC-GNs-Th-GOx and GC-GNs-Th-DGNs electrodes. Finally, the electrodes were tested successfully for selective recognition of glucose and nitrite, respectively.

2. Experimental section

2.1. Material and Reagents

Graphite powder (1 to 2 micron), $HAuCl_4 \cdot 3H_2O$, Th, GOx, (Aspergillus Niger 20,000 units/g, EC 1.1.3.4) and other chemicals were of analytical grade obtained from commercial sources (Sigma-Aldrich® or Merck®). All solutions were prepared with double-distilled water. Stoke solutions of 10 mM glucose and nitrite 30 mM were prepared in 0.1 M PBS, pH 7.0, and stored overnight at 4 ^{o}C under argon atmosphere before use.

2.2. Preparation of GC-GNs electrode

Graphene oxide (GO) was synthesized by the Hummer's method (Hummers and Offeman, 1958), partially modified in our group (Shervedani and Amini, 2014, see also Supporting Information, Section 1). The GC electrode (0.0314 cm^2) was cleaned by polishing with 1 and 0.3 μm alumina powder sequentially, and then, washed ultrasonically in ethanol and water for a few minutes, respectively.

A 20 mL mixture including 2.0 mg mL^{-1} GO was prepared in aqueous solution, stirred, and sonicated in an ultrasonic bath (Bandlin, HF 35 kHz) for 2h to prepare GO suspension solution for deposition. The GC-GNs electrode was prepared using clean GC electrode as follows:

A 20 μL sample of GO solution was dropped onto the clean GC electrode (or ITO) and dried under air to attach GO onto the GC surface, forming GC-GO (or ITO-GO) electrode. The electrochemical cell was filled with 0.1 M KNO_3 solution. The GC-GO electrode was placed into the cell, its potential was cycled, 20 mV s^{-1}, between 0.000 and −1.300 V vs. Ag/AgCl at room

temperature up to ~7 cycles to reduce GO to GNs (Lu et al., 2013), forming GC-GNs (or ITO-GNs) (Fig. S1, Supporting Information).

2.3. Preparation of GC-GNs-Th-GOx and GC-GNs-Th- DGNs electrodes

Amine diazonium cation was generated based on Belanger method (Lyskawa and Belanger, 2006) with some modifications in our group. The GC-GNs electrode surface was modified with Th via in-situ generated aryl diazonium cation based on electrochemical reduction of corresponding aniline function of Th in acidic media. Typically, 7.0 mg of Th was predissolved in 5 mL of 0.5 M HCl solution, and mixed with 3.5 mg sodium nitrite predissolved in 5 mL of double-distilled water. The mixture was degassed with argon and left at 0 °C for about 15 min to react and form diazotation mixture. The electrografting was immediately performed in the diazotation mixture on GC-GNs electrode surface by cycling the electrode potential between 0.000 to −0.800 V at 50 mV s^{-1} (four cycles). Formation of Th on GC-GNs electrode surface was completed after three cycles resulting GC-GNs-Th electrode. For the fabrication of GC-GNs-Th-GOx electrode, five μL of GOx solution (5 mg mL^{-1}) was coated onto the GCE-GNs-Th electrode surface and dried at 4 ^{o}C in air.

The GC-GNs-Th-DGNs electrode was prepared by electrodeposition of Au onto the GC-GNs-Th electrodes in 0.1 M H_2SO_4 aqueous solution containing 0.2 mM $HAuCl_4$ at −0.200 V for 90 s.

2.4. Apparatus and Physicochemical Characterization

X-ray photoelectron spectroscopy (XPS) analysis was carried out on a VG Microtech Twin anode XR3E2 X-ray source and a concentric hemispherical analyzer operated at a base pressure of 5×10^{-10} mbar using Al K_α ($h\nu = 1486.6$ eV). The XPS measurements have been performed on

the ITO-GO and ITO-GN samples. Field emission scanning electron microscopic (FESEM) images were acquired using a scanning electron microscope (SEM, Hitachi S4160, Cold Field Emission, Japan). Compositional analysis of the sample was completed by an Energy Dispersive X-ray (EDX) microanalyzer attached to the FESEM. Surface Raman spectra were collected on a SENTERRA Raman spectrometer using 745 nm laser excitation. All the electrochemical studies are performed at $25 \pm 2\ ^{\circ}C$ using a three-electrode assembly glass cell including, a Ag/AgCl (3 M KCl) electrode as reference electrode, a large area Pt as counter electrode (70 times larger than that of the working electrode), and the modified GC disk as working electrode. The cyclic voltammetry (CV) and electrochemical impedance spectroscopy (EIS) measurements were carried out on Autolab Potentiostat/Galvanostat101 instrument equipped with a frequency response analyzer, and controlled by Nova 1.8 Software (Eco Chemie, Utrecht, the Netherlands). The EIS data were approximated using ZView2.3f® software, considering the fit criteria and using appropriate electrical equivalent circuit built in this software, from which kinetic parameters were extracted (Shervedani et al., 2011).

3. Results and discussion

3.1. Fabrication of GCE-GNs and GCE-GNs-Th modified electrodes

Modifications of the surface are schematically represented in Scheme 1. (see Section 2.2, also Fig. S1).

Here Scheme 1

Surface morphology and topographical details of the GC-GO and GC-GNs electrodes were characterized by using FESEM (Fig. 1A and 1B) and EDX (Fig. S2, Supporting Information).

The shape of GNs and GO are regularly flake-like (like bride-white-dress) and slightly wrinkled, exhibiting many interlaced edges. A comparison between the EDX profile obtained on the GC-GO with that obtained on GC-GNs (Fig. S2 and Tables S1 and S2, Supporting Information) indicates a notable decrease in oxygen content, from 19.7 to 3.2 wt.%, implying that the oxygen functionalities are significantly decreased from GC-GO to GC-GNs electrodes.

Here Fig. 1

Surface Raman spectroscopy is a widely applied tool to characterize carbon products based on variations in the Raman intensities of the conjugated and double carbon−carbon bonds. The G and D bands of carbon products are assigned to the E_2g phonon of sp^2 carbon atom and the breathing mode of K-point phonons of A_1g symmetry, respectively (Kudin et al., 2008; Raj and John, 2013). The Raman spectra of the ITO/GO and ITO/GNs are shown in Fig. 2A.

The GO is characterized by typical bands, D band at 1320 cm^{-1} and G-band at 1590 cm^{-1}, which are representatives of sp^3 and sp^2 carbon hybridization, respectively (Graf et al., 2007; Stankovich et al., 2007). After the electrochemical reduction of GO to GNs, the intensity of D-band is increased, and the G-band place is shifted to lower frequency region (1579 cm^{-1}), supporting the reduction of GO to GNs (Stankovich et al., 2007).

The XPS measurements were performed to trace electrochemical reduction of GO to GNs. Figs. 2B and 2D show the XPS survey spectrum of ITO-GO and ITO-GNs-Th electrodes.

Here Fig. 2

The peak observed at 284.5 eV corresponds to the C1s of sp^2 carbon (Graf et al., 2007), and that observed at 531 eV corresponds to the O1s of various oxygen functional groups. The intensity ratio of C/O peaks was calculated as 1.61 (Fig. 2B). After electrochemical reduction of GO attached onto ITO substrate, the XPS spectrum showed a significant variation in the C/O intensity ratio of the peaks of C1s and O1s. Namely, the C/O intensity ratio has been increased from 1.61 to 4.82 upon electrochemical reduction of ITO-GO to GNs-modified ITO (Fig. 2D). This is due to the removal a significant fraction of oxygen functional groups from the surface of GO.

The high-resolution C1s XPS spectra ITO-GO (Fig. 2C) is fitted with different components of oxygen-containing functional groups: nonoxygenated C at 286.6, epoxy carbon at 288.8 eV, carbonyl carbon at 288.7 eV (Wang et al., 2011). The presence of a C-N bond was also detected at approximately 287.7 eV, which is of a higher energy than the C-O interaction (Fig. 2E). The presence of the C-N peak indicates that the N covalently bonded to the GC-GNs, and thus, supports successful incorporation immobilization of Th into the exfoliated GNs.

In addition, the N1s spectra (Fig. 2F) shows a two broad peaks at the positions of 399.8 and 399.6 eV, indicating the presence of two types of N bonding interaction in the structure of ITO-GNs-Th (Xu at al., 2008).

The Th molecules were grafted onto the GC-GNs surface by a simple electrochemical reduction process (Liu et al., 2011). The XPS spectrum of the ITO-GNs-Th electrode did not show significant difference with ITO-GNs, except the appearance of small peak at 405 eV (Fig. 2C), which could be due to the amine functionality of Th (for clarity only the spectrum of ITO-GNs-Th is presented).

Consecutive CVs recorded, in the range of 0.000 to −0.800 V vs. Ag/AgCl, during attachment of Th onto the GC, GC-GO and GC-GNs electrodes are presented in Fig. S3. The first CV recorded during attachment of Th onto the GC-GNs surface shows a broad irreversible wave located around −0.30 V (Fig. S3-C). The CV currents are significantly decreased upon recording the second CV, indicating passivation of the GNs surface by formation (electrografting) a monolayer of Th on the surface(please note that the electrografted Th is not electroactive in this potential window, see Section 3.2).

The broad irreversible waves observed on GC-Th and GC-GO-Th electrodes are located almost around −0.50 V, indicating that electrochemical reduction/adsorption of Th diazonium cation on GC-GNs electrode is shifted to more facile direction by almost a value of 0.200 V, compared with GC and GC-GO electrodes. More facile attachment of the Th on the GNs can be due to high reactivity of the edge sites of GNs layers toward Th.

The GC-GNs-Th surface (Fig. 1C) exhibits a wrinkle-like thin sheet (like mother-bride-gray-dress), which should be an interesting feature of GNs structure for next steps of the modifications, attachment of GOx or DGNs.

3.2. Determination surface concentration of immobilized thionine by CV and EIS

Surface concentration of attached Th on the GC-GNs-Th electrode is determined by CV and supported by the EIS findings. The CVs obtained in Ar-saturated 0.1 M PBS, pH 7.0 on GCE after each step of modification in the potential region of −0.300 to +0.300 V vs. Ag/AgCl where Th is electrochemically active (Unnikrishnan et al., 2013), are presented in Fig. S4. While the CVs obtained on GC and GC-GNs electrodes (curve a and b) are featureless, the GC-GNs-Th electrode displays a wide redox wave (curve c) around the potential of −0.060 V with relatively

large currents, which can be attributed to the confined redox reaction of the Th attached onto the GC-GNs surface. A reversible redox wave with smaller currents is observed for GC-Th electrode. The peak current obtained on the GC-GNs-Th electrode is almost 12 times larger than that obtained on GCE-Th electrode. This behavior is attributed to (i) the high reactivity of the edge sites and (ii) large surface area of GNs, in comparison with GC-based electrode; allow loading more Th molecules to be ordered on the GC-GNs electrode surface.

The surface concentration of Th on GC-Th and GC-GNs-Th electrode (Γ_{Th}) can be obtained by using CV and EIS methods, where $\Gamma_{Th,CV} = Q_{cv}/nFA$ and $\Gamma_{Th,EIS} = 4RTC_{\varphi}/n^2F^2A$ (Kudin et al., 2006). Values of 1.23×10^{-10} and 14.9×10^{-10} mol cm^{-2} are obtained for $\Gamma_{Th,CV}$, and 1.11×10^{-10} and 14.1×10^{-10} mol cm^{-2} for $\Gamma_{Th,EIS}$ on GC-Th and GC-GNs-Th electrodes, respectively (Figs. S4 and S5, and Table S3, Supporting Information). The EIS results are in good agreement with voltammetric findings, and both indicate that the value of Th immobilized on GC-GNs electrode is ~12 times larger than that immobilized on GC electrode. The GC-GNs-Th electrode is further modified and tested for biosensing applications.

3.3. Biosensing applications and analytical performance

Two sets of the GC-GNs-Th electrodes are prepared, modified further by GOx and DGNs separately, and tested for determination of biological species, glucose (Unnikrishnan et al., 2013) and nitrite (Ding and Wang, 2010)

3.3.1. Application for sensing of glucose

3.3.1.1. Direct electrochemistry of GOx immobilized as the GC-GNs-Th electrode

A glucose biosensor can be developed using GC-GNs-Th electrode modified based on electrostatic adsorption of negatively charged GOx on positively charged functions of Th (Shams and Nasri, 2013) at these conditions (Scheme 1).

The CVs obtained on GC-GNs (a), GC-GNs-Th (b), GC-GNs-GOx (c) and GC-GNs-Th-GOx (d) electrodes in 0.1 M PBS, pH 7.0, Ar-saturated at a scan rate of 50 mVs^{-1} in the potential window of –0.800 to –0.200 V, where GOx is electroactive, are presented in Fig. 3A. Three points should be explained here.

(i) While no faradaic current was observed for the CVs recorded on the GC-GNs (curve a) and GC-GNs-Th electrodes (curve b), a well-defined quasi-reversible redox wave is observed on the CVs of GC-GNs-GOx and GC-GNs-Th-GOx electrodes (curves c and d). Since no redox probe exists in the solution phase (also adsorbed Th is not electroactive in this potential window), the redox currents of the GC-GNs-Th-GOx should be ascribed only to the redox reaction of the immobilized GOx, i.e. to $FAD + 2H^+ \leftrightarrow H_2FAD$. The control experiments revealed no significant adsorption of GOx on GC and GC-Th electrodes.

Here Fig. 3

(ii) The behavior of GC-GNs-GOx electrode ($E^{0\prime} = -0.520$ V and $\Delta E_p = 0.062$ V, Fig. 3A, curve c) are close to those previously reported (Unnikrishnan et al., 2013) on similar modified electrode (GCE/RGO-GOx), however, the activities of GC-GNs-Th-GOx electrode ($E^{0\prime} = -0.046$ V and $\Delta E_p = 0.039$ V, curve d) are significantly improved, displaying more reversible behavior. Notably, the peak current (I_p) observed on GC-GNs-Th-GOx electrode is considerably (~3.5 times) larger than that observed on GC-GNs-GOx electrode (curve c). The

enhanced redox peak current is attributed to larger amount of GOx molecules immobilized on GC-GNs-Th, and the smaller value of ΔEp to the efficient interaction and faster electron transfer between the enzyme and GC-GNs-Th platform, which may be called synergetic effect of surface and subsurface (Mu et al., 2011, Zhang et al., 2015). This is an interesting feature, demonstrating ability of the modifying film GNs-Th for immobilization and direct electron transfer of GOx at the GC electrode surface.

(iii) Although adsorption of GOx onto the electrode is implicitly understood from the above discussion, the CV experiments were performed to further support this behavior. For details, variations of I_p vs. scan rate (Fig. S6), please see Supplementary Information, Section 6.

3.3.1.2. Analytical performance of GC-GNs-Th-GOx for glucose

The CVs obtained on the GC-GNs-Th-GOx as a function of glucose concentrations added into the testing cell solution (Fig. 3B) show that I_{pc}, related to the reduction of O_2, is decreased by increasing the glucose concentration. The dynamic calibration curve extracted from CV responses against glucose concentration shows a linear behavior, ranging from 0.5 to 6.0 mM glucose [as $I_p/\mu A = 1.2\ C_{glucose/}mM + 0.83$, $R^2 = 0.9866$], with a sensitivity of 43.2 $\mu A\ cm^{-2}\ mM^{-1}$, and the limit of detection (LOD) of 9.6± 0.42 μM, where the LOD is evaluated for linear range based on signal = 3σ, and σ is standard deviation for (n = 5) measurements on the GC-GNs-Th-GOx electrode in blank reagent testing solution. A comparison between the results obtained by using the currently designed biosensor with those reported on GNs-based electrodes (Table S4, Supporting Information) indicates that the sensitivity and detection limit of glucose in the present work are significantly improved.

3.3.2. Modification of GC-GNs-Th with DGN for sensing of $NO2^{-}$

Determination of nitrite ion (NO_2^-) is of great importance since nitrite is widely used in the environment, beverages, and food products as a preservative (Ding and Wang, 2010). Analytical methods developed for determination of nitrite ion are mainly based on spectrophotometry (Kuznetsov and Zemyatova, 2010), separation and chromatography (Michalski and Kurzyca, 2006) and electrochemistry (Yue et al., 2011) techniques, however electrochemical techniques are preferred because of their several advantages (Kozub et al., 2010, see also Supporting Information, Section 7).

3.3.2.1. Characterization the GC-GNs-Th-DGNs electrode

(i) Topographical microanalysis; The micrographs of the modified electrode (Fig. 1E) indicates that electrodeposited gold forms relatively large dendrite-like nanostructures, DGNs (with length ~1 μm and diameters up to hundreds of nanometers), on GC-GNs-Th surface which are uniformly distributed; however the gold deposited on the GC-GNs surface forms small nanoparticles, AuNPs (with average diameter of ~65 nm), also uniformly distributed. These results clearly demonstrate that the GNs-Th has a crucial effect on the morphology of the surface. A typical EDX spectrum obtained on the surface of GC-GNs-Th-DGNs electrode is presented in Fig. 1F, supporting the presence of DGNs (similar effect observed for AuNPs). The growth of DGNs on the surface of the GC-GNs-Th electrode is expected to increase the number of active sites and enhance the electrochemical activity of the surface towards electro-oxidation of nitrite.

(ii) Electrochemical characterization; To support the presence of Au on the modified electrodes and estimate number of Au active sites (Γ_{Au}), potential of the GC-GNs-AuNPs and GC-GNs-Th-DGNs electrodes were cycled between 0.000 to +1.500 V vs. Ag/AgCl in

0.05 M sulfuric acid aqueous solution, where gold could be subjected to redox reaction. The steady-state voltammograms obtained on the studied electrodes are presented in Fig. S7. Values of 1.30×10^{-10} mol cm^{-2} and 5.2×10^{-10} mol cm^{-2} were obtained for Γ_{AuNPs} and Γ_{DGNs} based on $\Gamma = Q/nF$, where Q is the charge obtained from the area of the reduction peak observed around +0.800 V, and n = 2 based on AuO/Au redox reaction (Hoare, 1984).

The results show that not only the size and arrangement of the gold nanoparticles formed on these platforms, GC-GNs-AuNPs and GC-GNs-Th-DGNs, are different (Fig. 1E), but also the number of Au active sites (Γ_{Au}) of these electrodes are different [($\Gamma_{DGNs}/\Gamma_{AuNPs}$) = 4]. Therefore, we expect to observe different electrocatalytic for these electrodes toward oxidation of NO_2^- ion.

3.3.2.2. Electrocatalytic activity of GC-GNs-Th-DGNs for oxidation of NO_2^-

The CVs obtained on (a) blank (GC-GNs-Th, PBS, pH 7.4, without NO_2^-), (b) GC, (c) GC-GNs, (d) GC-GNs-Th, (e) GC-GNs-AuNPs and (f) GC-GNs-Th-DGNs electrodes in presence of 1.0 mM nitrite are presented in Fig. 4A. The GC-GNs-Th-DGNs electrode shows a well-defined peak at +0.760 V for oxidation of nitrite, which is shifted by 90 mV to more facile direction (less positive potentials) compared with GC-GNs-Th electrode. Moreover, nitrite oxidation peak current observed at GC-GNs-Th-DGNs electrode is larger than that observed at GC-GNs-AuNPs and GC-GNs-Th electrodes. Both effects, decrease in the overpotential and increase in the current, indicate an electrocatalytic activity for the modified electrode towards oxidation of nitrite which is attributed to the presence Au on GC-GNs-Th-DGNs structure.

3.3.2.3. Analytical performance of GC-GNs-Th-DGNs for NO_2^-

After optimization of the experimental conditions, nitrite was amperometrically detected on GC-GNs-Th-DGNs electrode. The electrode responded quickly to the oxidation of nitrite in a wide range of concentrations, monitored for successive additions of nitrite to the test solution (Fig. 4B). Accordingly, a wide dynamic range calibration curve varied from 0.05 to 1.0 mM with two linear parts, from 0.05 to 1.0 μM NO_2^- [as $I_p(\mu A) = 262.3[NO_2]/mM + 2.1$, $R^2 = 0.9941$] and from 30.0 to 1000.0 μM NO_2^- [as $I_p(\mu A) = 100.1[NO_2]/mM + 3.6$, $R^2 = 0.9976$] and sensitivities of 262.3 μA mM^{-1} and 100.1 μA mM^{-1} (Fig. 4B, inset) is obtained. The LOD evaluated for the lower linear range was 0.01 μM for (n = 5) measurements. The analytical characteristics of the method are compared with those previously reported for nitrite sensors, (Table S5, Supporting Information). Excellent electrochemical properties of the GC-GNs-Th-DGNs electrode toward the oxidation of NO_2^- can be attributed to the large surface area and the special three-dimensional assembly of DGNs, compared with simple AuNPs formed on GC-GNs- AuNPs electrodes.

Here Fig. 4

3.3.2.4. Interference study

Influence of the potential interferences on the determination of nitrite (Ding and Wang, 2010; Radhakrishnan et al., 2014) is evaluated by the amperometric method at $E_{DC} = 0.860$ V and applying the method of mixed solutions. The results show that the GC-GNs-Th-DGNs electrode exhibits well-defined amperometric response toward 0.5 mM NO_2^- without remarkable amperometric response for the additions of 1.0 mM of possible interferences, including Ca^{2+}, Mg^{2+}, Cu^{2+}, F^-, Br^-, IO_3^- and SO_4^{2-}(Fig. S8, Supporting Information).

3.4. Reproducibility and repeatability of GC-GNs-Th-GOx and GC-GNs-Th-DGNs electrodes

Reproducibility of the electrodes are investigated by recording the response of four identically prepared electrodes made of each type of materials, GC-GNs-Th-GOx and GC-GNs-Th-DGNs, and measured individually in the separate solutions of 1.5 mM glucose and 0.5 mM nitrite, respectively. The small relative standard deviations (RSDs) of 3.9% and 2.8% indicate high reproducibility of the method for preparation of GC-GNs-Th-GOx and GC-GNs-Th-DGNs electrodes, respectively. The repeatability of the electrodes is also verified. A set of five consecutive measurements is performed for one of the electrode of each type in 1.5 mM glucose and nitrite separate solutions. The obtained results with RSD of 3.1% and 2.3% demonstrate excellent repeatability for GC-GNs-Th-GOx and GC-GNs-Th-DGNs electrodes, respectively.

3.5. Applicability of GC-GNs-Th-GOx and GC-GNs-Th-DGNs electrodes

Applicability of the modified electrodes was tested by determination of (i) glucose in human blood serum samples on the GC-GNs-Th-GOx electrode, and (ii) nitrite in river water and mineral water samples GC-GNs-Th-DGNs, based on addition/recovery tests and utilization of the calibration curve method. The results are summarized in Table 1, supporting applicability of the modified electrodes for determination of glucose and nitrite ion in real samples.

Here Table 1

4. Conclusions

Two types of nanomaterials were synthesized on the GC electrode surface by using thionine (Th), electrografted onto graphene nanosheets (GNs) via its diazonium salt, and then, decorated via

(i) electrostatic attachment of glucose oxidase (GOx) and (ii) electrodeposition of gold dendrite-like nanostructures. The fabricated electrodes, GC-GNs-Th-GOx and GC-GNs-Th-DGNs, were successfully tested for determination of glucose and NO_2^- ion, respectively.

(i) A sensitivity of 43.2 μA cm^{-2} mM^{-1} and detection limit of 9.6 μM M glucose was obtained based on direct electron transfer at the GC-GNs-Th-GOx electrode.

(ii) Also, a sensitivity of 262.3 μA mM^{-1} and detection limit of 0.010 μM NO_2^- was obtained based on oxidation of NO_2^- at the GC-GNs-Th-DGNs electrode.

Applicability of the (i) GC-GNs-Th-GOx and (ii) GC-GNs-Th-DGNs electrodes was supported by results obtained for determination of (i) glucose in blood serum and (ii) nitrite ion in water samples, respectively.

Acknowledgment

The authors gratefully acknowledge the University of Isfahan for financial supports and research facilities.

References

Belanger, D., Pinson, J., 2011 Chem. Soc. Rev. 40, 3995–4048.

Brooksby, P.A., Downard, A.J., Yu, S.S.C., 2005. Langmuir 21, 11304–11311.

D'Amours, M.; Belanger, D., 2003. J. Phys. Chem. B 107, 4811–4817.

Deng, C., Chen, J., Nie, Z., Yang, M., Si, S., 2012. Thin Solid Films 520, 7026–7029.

Ding, Y., Wang, Y., Lei, Y., 2010. Biosens. Bioelectron. 26, 390–397.

Gao, Q., Cui, X., Yang, F., Ma, Y., Yang, X., 2003. Biosens. Bioelectron. 19, 277–282.

Gautham, K.A., Chanchal, K.M., 2010. Biosens. Bioelectron. 25, 2016-2020.

Geim, A.K., 2009. Science, 324, 1530-1534.

Georgakilas, V., Otyepka, M., Bourlinos, A.B., Chandra, V., Kim, N., Kemp, K.C., Hobza, P., Zboril, R., Kim, K.S., 2012. Chem. Rev. 112, 6156–6214.

Ghica, M.E., Ferreira, G.M., Brett, C.M.A., 2015, J Solid State Electrochem. 19, 2869-2881.

Gooding, J.J., Ciampi, S., 2011. Chem. Soc. Rev. 40, 2704-2718.

Graf, D., Molitor, F., Ensslin, K., Stampfer, C., Jungen, A., Hierold, C., Wirtz, L., 2007. Nano Lett. 7, 238-242.

Guo, L., Zhang, Q., Huang, y., Han, Q., Wang, Y., Fu, Y., 2013. Bioelectrochemistry 94, 87-93.

Hetemi, D., Kanoufi, F., Combellas, C., Pinson, J., Podvoric, F.I., 2014. Langmuir 30, 13907-13913.

Hoare, J.P., 1984. J. Electrochem. Soc. 131, 1808–1815.

Hummers, W.S., Offeman, R.E., 1958 J. Am. Chem. Soc. 80, 1339.

Kozub, B.R., Rees, N.V, Compton, R.G., 2010. Sens. Actuators, B 143, 539-546.

Kudin, K.N., Ozbas, B., Schniepp, H.C., Prudhomme, R.K., Aksay, I.A., Car, R. 2008. Nano Lett. 8, 36−41.

Kuila, T. Bose, S., Mishra, A.K., Khanra P., Kim, N.H., Lee, J.H., 2012. Prog. Mater. Sci. 57, 1061–1105.

Kuznetsov, V.V., Zemyatova, S.V., 2010. J. Anal. Chem. 62, 637–644.

Lange, U., Hirsch, T., Mirsky, V.M., Wolfbeis, O.S., 2011. Electrochim. Acta 56, 3707-3712.

Li, X., Wang, X., Zhang, L., Lee, S., Dai, H., 2008. Science 319, 1229-1232.

Li, X., Zhu, Y., Cai, W., Borysiak, M., Han, B., Chen, D., Piner, R.D., Colombo, L., Ruoff, R.S., 2009. Nano Lett. 9, 4359-4363.

Ling, X., Xie, L.M., Fang, Y., Xu, H., Zhang, H.L., Kong, J., Dresselhaus, M.S., Zhang, J., Liu, Z.F., 2010. Nano Lett. 10, 553-561.

Liu, G., Luais, E., Gooding, J.J., 2011. Langmuir 27, 4176-4183.

Liu, X.Q., Zhang, J.M., Liu, S.H., Zhang, Q.Y., Liu, X.H., Wong, D.K.Y., 2013. Anal. Chem. 85, 4350-4356.

Lu, L., Zhang, O., Xu, J., Wen, Y., Duan, X., Yu, H., Wu, L., Nie, T., 2013. Sens. Actuators, B 181, 567-574.

Lyskawa, J., Belanger, D., 2006. Chem. Mater. 18, 4755-4763.

Michalski, R., Kurzyca, I., 2006. Pol. J. Environ. Stud. 15, 5-18.

Mu, R., Fu, Q., Xu, H., Zhang, H., Huang, Y., Jiang, Z., Zhang, S., Tan, D., Bao, X., 2011. J. Am. Chem. Soc. 133, 1978–1986.

Novoselov, K.S., Morozov, S.V., Jiang, W., Zhang, Y., Dubonos, S.V., Grigorieva, I.V., Firsov, A.A., 2004. Science 306, 666-669.

Portaccioa, M., Tuoro, D.D., Arduinic, F., Mosconec, D., Cammarota, M., Mita, D.G., Lepore, M., 2013. Electrochimica Acta, 109, 340 347.

Radhakrishnan, S., Krishnamoorthy, K., Sekar, C., Wilson, J., Kim, S. 2014. Appl. Catal. B: Environ. 148, 22– 28.

Raj, M.A., John, S.A., 2013. J. Phys. Chem. C 117, 4326-4335.

Shams, E., Nasri, Z., 2013. Electrochim. Acta 112, 640–647.

Shervedani, K.R., Akrami, Z., Sabzyan, H., 2011. J. Phys. Chem. C 115, 8042-8055.

Shervedani, R.K., Amini, A., 2014. Electrochim. Acta 142, 51–60.

Stankovich, S., Dikin, D.A., Piner, R.D., Kleinhammes, K.A., Jia, Y., Wu, Y., Nguyen, S.B.T., Ruoff, R.S., 2007. Carbon 45, 1558-1565.

Unnikrishnan, B., Palanisamy, S.S., Chen, M., 2013. Biosens. Bioelectron. 39, 70–75.

Wang, L., Luo, J., Schadt, M.J., Zhong, C.J., 2009. Langmuir 26, 618-632.

Wang, S., Yu, D., Dai, L., Chang, D.W., Baek, J.B. 2011. ACS Nano 5, 6202-6209.

Xu, F.; Minniti, M.; Barone, P.; Sindona, A.; Bonanno, A.; Oliva, A. 2008. Carbon 46, 1489-1496.

Yin, P.T., Shah, S., Chhowalla, M., Lee, K.B., 2015, Chem. Rev. 115, 2483–2531.

Yue, R., Lu, Q., Zhou, Y.K., 2011. Biosens. Bioelectron. 26, 4436–4441.

Zhang, W., Li, Y., Zeng, X., Peng, S., 2015, Nature, Doi: 10.1038/srep10589.

Zhu, L., Luoa, L., Wang, Z., 2012. Biosens. Bioelectron. 35, 507-511.

Research Highlights

- Thionine is grafted to GC-GNs & decorated with (i) GOx enzyme or (ii) nano-dendritic gold.
- The GC-GNs-Th-GOx & GC-GNs-Th-DGNs electrodes are tested for biosensing intentions.
- Glucose in blood serum and nitrite in water are determined successfully using these sensors.
- Step-by-step of the work is traced by CV, EIS, SEM-EDX, Raman and XPS methods.

Table 1. Results obtained for practicality of GC-GNs-Th-GOx for determination of glucose in human blood serum and GC-GNs-Th-DGNs for determination of nitrite in rainwater and river samples. Results are average of 4 measurements in each case.

Sample	Added (mM)	Founded (mM)	RSD (%)	Recovery
Serum sample	___	0.400	3.9	___
Sample 1	0.5	0.910	3.4	101.1
Sample 2	0.5	1.380	4.1	98.5
Sample 3	0.5	1.870	3.3	98.4
Mineral sample	___	0.0030	2.1	___
Sample 1	0.0050	0.0078	2.9	97.5
Sample 2	0.0050	0.0131	2.6	102.3
River sample	___	0.0050	2.3	___
Sample 1	0.0050	0.0099	3.2	99.0
Sample 2	0.0050	0.0148	2.6	98.6

Figure Captions

Scheme 1. Schematic representation for the fabrication of the GC-GNs, GC-GNs-Th, GC-GNs-Th-GOx and GC-GNs-Th-DGNs electrodes.

Figure 1. FESEM micrographs obtained on the (A) GC-GO, (B) GC-GNs, (C) GC-GNs-Th, (D) GC-GNs-AuNPs, (E) GC-GNs-Th-DGNs electrodes. (F) EDX patterns obtained on the GC-GNs-Th-DGNs electrode.

Figure 2. (A) Raman spectra obtained on the surface of (a) ITO/GO and (b) ITO/GNs electrodes using 745 nm laser excitation. (B) Survey XPS spectra obtained in the region of 0.0 to 1200.0 eV on the surface of ITO/GO, (C) High-resolution C1s spectra region of the ITO/GO, (D) the survey-scan XPS spectra obtained in the region of 0.0 to 1200.0 eV on the surface of ITO/GNs-Th electrodes, (E) and (F) High-resolution C1s and N1s spectra region of the ITO/GNs-Th respectively.

Figure 3. (A) The CVs of (a) GC-GNs, (b) GC-GNs-Th, (c) GC-GNs-GOx and (d) GC-GNs-Th-GOx in N_2-saturated 0.1 M PBS, pH 7.4 at scan rate of 50 mV s^{-1}. (B) The CVs obtained on the GC-GNs-Th-GOx as a function of glucose concentrations added into the testing cell solution, 0.1 M PBS, pH 7.4, saturated with oxygen. Inset shows linear variation of $I_{p,c}$ vs. glucose concentration.

Figure 4. (A) The CVs obtained on (a) blank (GC-GNs-Th, cell solution without nitrite), (b) GC, (c) GC-GNs, (d) GC-GNs-Th, (e) GC-GNs-AuNPs and (f) GC-GNs-Th-DGNs electrodes, cell solution containing PBS, pH 7.0, 1.0 mM nitrite, scan rate: 50 mV s^{-1}. (B) Chronoamperometric response of the GC-GNs-Th-DGNs electrode at +0.86 V upon successive addition of nitrite into 0.1 M PBS, pH 7.0 under a constant-rate stirring. The insets show amperometric responses of the electrode at low (B-a) and high (B-a) concentrations of nitrite ion.

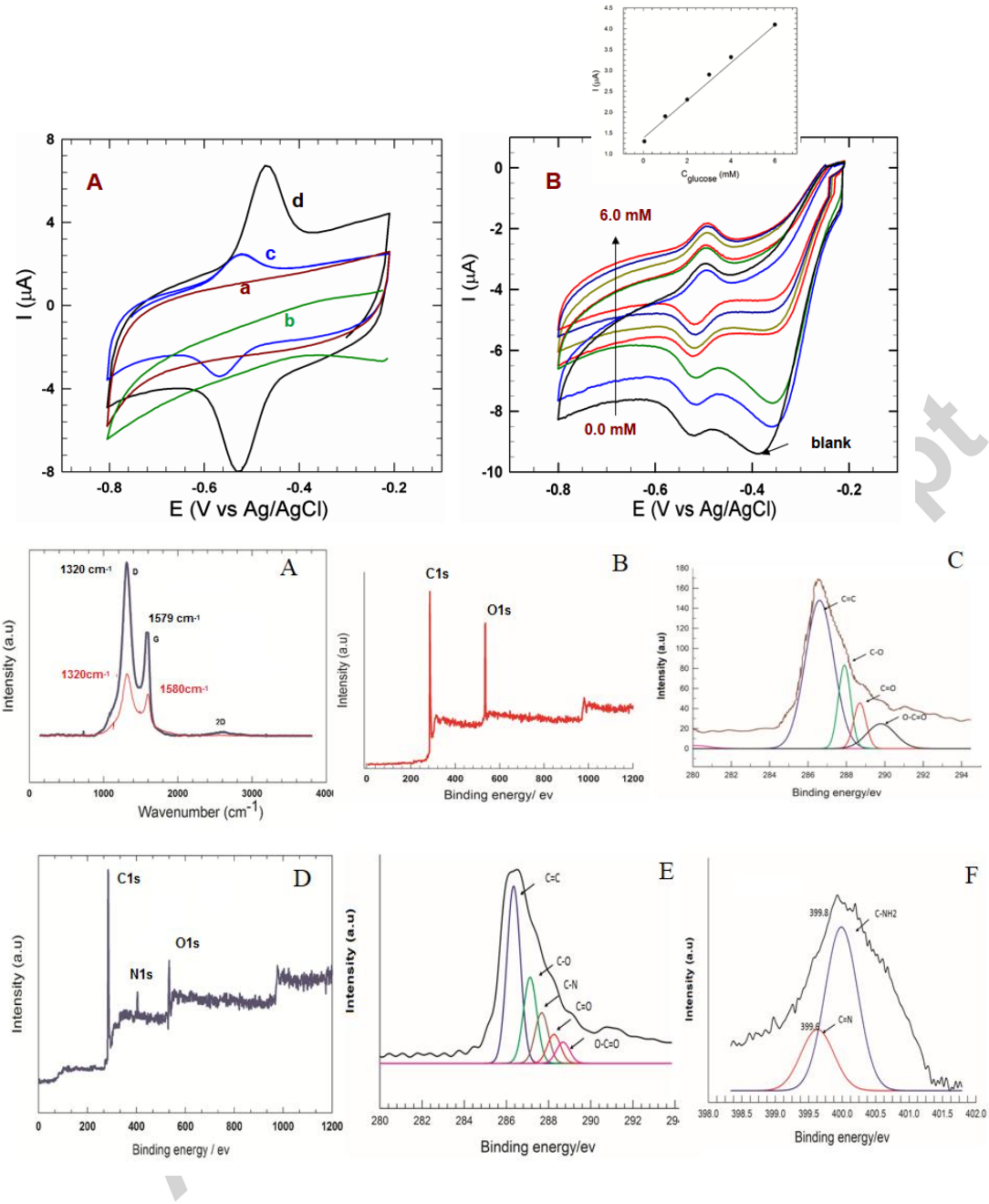
A
d
c
a
b
I (μA)
E (V vs Ag/AgCl)
B
6.0 mM
0.0 mM
blank
I (μA)
E (V vs Ag/AgCl)
I (μA)
C_glucose (mM)
A
1320 cm-1
1579 cm-1
1320cm-1
1580cm-1
Intensity (a.u)
Wavenumber (cm-1)
B
C1s
O1s
Intensity (a.u)
Binding energy/ ev
C
C=C
C-O
C=O
O-C=O
Intensity (a.u)
Binding energy/ev
D
C1s
O1s
N1s
Intensity (a.u)
Binding energy / ev
E
C=C
C-O
C-N
C=O
O-C=O
Intensity (a.u)
Binding energy/ev
F
399.8
C-NH2
399.6
C=N
Intensity (a.u)
Binding energy/ev

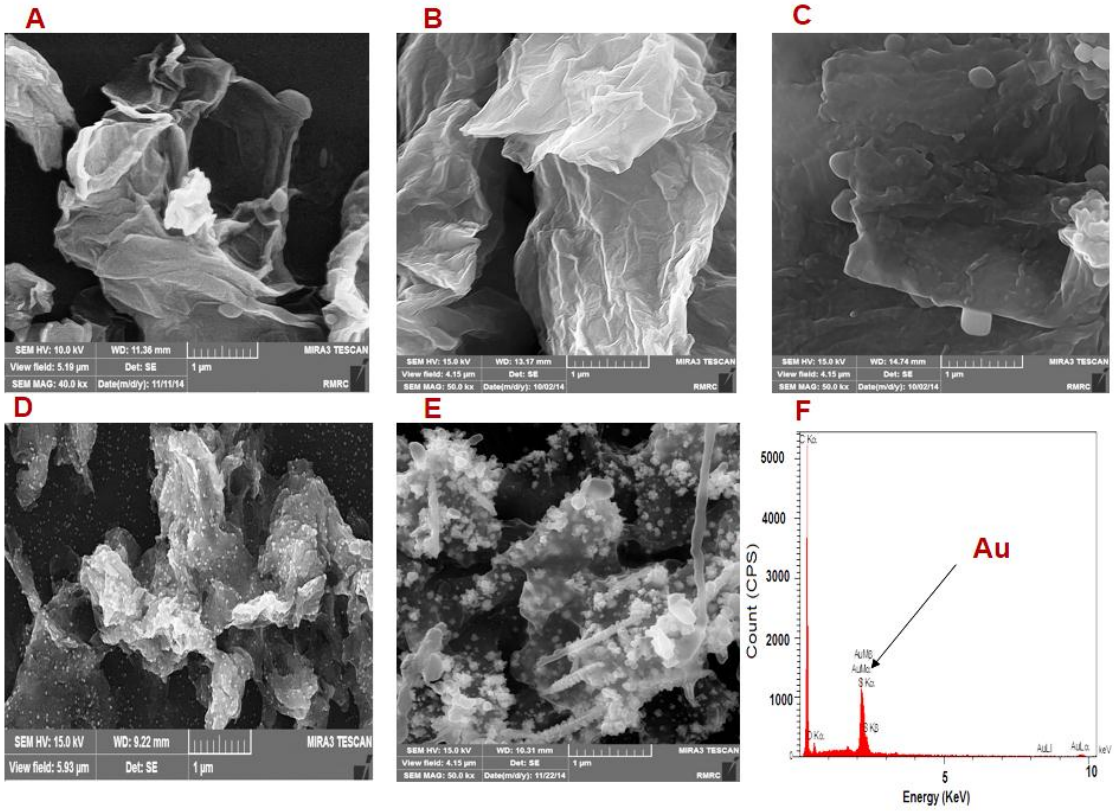
A
B
C
D
E
F
Au
Count (CPS)
Energy (KeV)

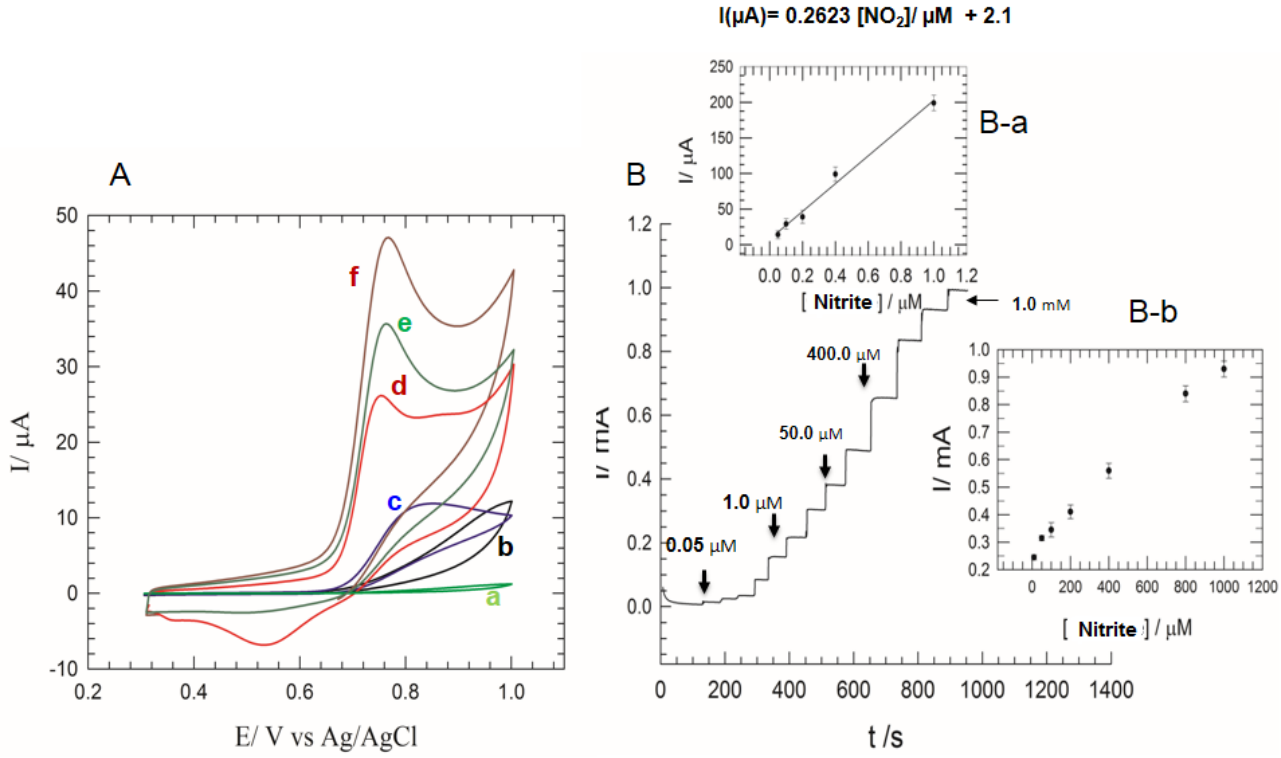
I(μA)= 0.2623 [NO2]/ μM + 2.1
A
I/ μA
E/ V vs Ag/AgCl
f
e
d
c
b
a
B
B-a
B-b
I/ μA
[Nitrite] / μM
1.0 mM
400.0 μM
50.0 μM
1.0 μM
0.05 μM
I/ mA
t /s